

Hotspots, mantle plumes and core heat loss

Stéphane Labrosse^{*,1}

Institut de Physique du Globe de Paris, 4 place Jussieu, 75252 Paris Cedex 05, France

Received 3 July 2001; received in revised form 7 February 2002; accepted 12 February 2002

Abstract

The heat flux at the core–mantle boundary (CMB) is a key parameter for core dynamics since it controls its cooling. However, it is poorly known and estimates range from 2 TW to 10 TW. The lowest bound comes from estimates of buoyancy fluxes of hotspots under two assumptions: that they are surface expression of mantle plumes originating from the base of the mantle, and that they are responsible for the totality of the heat flux at the CMB. Using a new procedure to detect plumes in a numerical model of Rayleigh–Bénard convection (convection between isothermal horizontal planes) with internal heating, it is shown that many hot plumes that start from the bottom boundary do not reach the top surface and that the bottom heat flux is primarily controlled by the arrival of cold plumes. Hot plumes easily form at the bottom boundary but they are mostly due to the spreading of cold plume heads that allow the concentration of hot matter. These plumes are generally not buoyant enough to cross the whole system and the hot plumes that reach the top surface result from an interaction between several hot plumes. According to this simple dynamical behavior, the heat flux at the bottom boundary is shown to be strongly correlated with the advection due to cold plumes and not with advection by hot plumes that arrive at the surface. It is then inferred that the heat flux out of hotspots can only give a lower bound to the heat flow at the CMB and that knowing the advection by subducted plates would give a better estimate. © 2002 Elsevier Science B.V. All rights reserved.

Keywords: convection; plumees; dynamics; heat flux; heating

1. Introduction

The plume model of Morgan [1] to explain alignments of intra-plate volcanoes – known as hotspots – is widely accepted. Mantle plumes are then seen as objects largely independent of

plates and large-scale mantle circulation and carrying heat and isotopes from their source (D'' or any internal boundary layer) to the surface (e.g. [2,3]). The total heat flow coming out of hotspots [4,5] is often interpreted as the total heat loss of the core. However, plume dynamics in high Rayleigh number convection [6–8] are very different from the dynamics of isolated plumes over fixed sources (e.g. [9–12]) which are forced to rise owing to their continuous supply of buoyancy. In particular, when convection is partially driven from volumetric heat sources – like mantle convection with radioactive heating – hot plumes, though easily formed, do not often reach the top surface

* Tel.: +33-1-44-27-49-35; Fax: +33-1-44-27-49-32.
E-mail address: labrosse@ipgp.jussieu.fr (S. Labrosse).

¹ Part of this paper was prepared at the department of Earth and Space Sciences, University of California, Los Angeles.

[7]. Heat transported by these plumes that are seen at the surface can therefore not be a correct estimate of core heat loss even in a mantle without any additional complexity such as chemical or phase stratification and even without taking into account filtering by the lithosphere [13].

On the other hand, there is another way of removing heat from the core than starting hot plumes: the arrival and spreading of cold plates [14,15]. The respective proportions of these two mechanisms are not known but are investigated in this paper, using a simple convection model and a new procedure for automatic, real-time, plume detection. It will be shown in this paper that cold plumes are the dominant heat transfer mechanism in convection that is partially internally heated, even close to the bottom boundary.

2. Detecting plumes in a convection model

The convection model used in the present study has been presented elsewhere [7] and only the main lines will be briefly recalled here. The conservation equations for momentum, energy and mass in the Boussinesq approximation are solved using a finite difference formulation. The top and bottom surfaces of the system are free-slip and held at constant temperature. In addition to this classic Rayleigh–Bénard setting, the system is uniformly heated from within. This system is then

entirely controlled by two non-dimensional parameters: Ra , the classical Rayleigh number for convection between horizontal plates at fixed temperatures (e.g. [16]), and H , the non-dimensional internal heating rate [7]. An important feature of the model is its three-dimensionality. In two-dimensional models, each plume represents an important fraction of the total volume of the system and depletes a large proportion of the boundary layer. When dealing with heat transport by plumes, it is of particular importance that the plumes are cylindrical and not two-dimensional.

For sufficiently high Ra , the system is fully time-dependent and the time evolution is due to the intermittent formation of plumes, their mutual interaction leading to their merging [10], and the formation of new plumes in the space left available [6–8,17]. The results presented here are obtained for $Ra = 10^7$ and $H = 20$, resulting in a bottom heat flux that is about 50% of the surface heat flux. A snapshot of the temperature field in the domain is represented in Fig. 1A using two iso-surfaces of different temperatures. On the right corner, a cold plume forms an arch, which shows that the plume results from the merging of two plumes. To study quantitatively this type of dynamics, we need to detect automatically the plumes during the course of the model computation.

Plumes are detected in the temperature field making use of their anomalous temperature, hot-

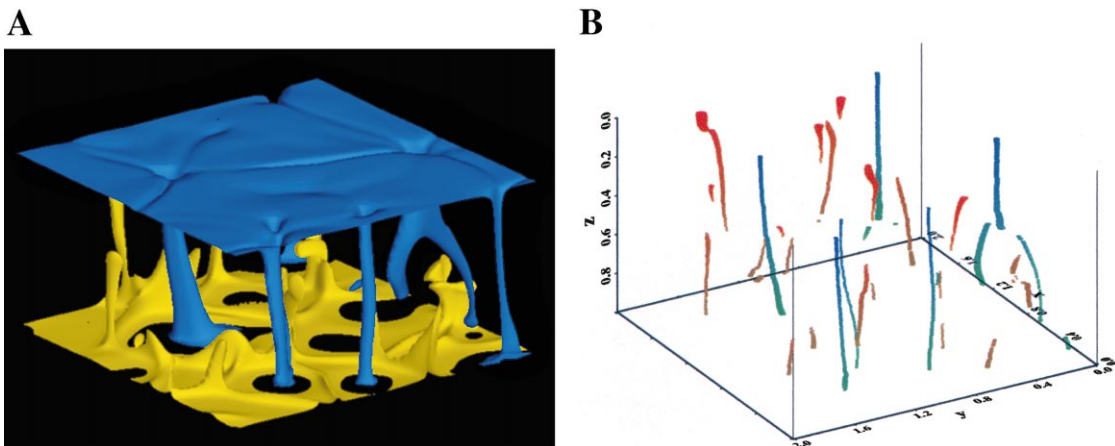


Fig. 1. Snapshot of the temperature field for $Ra = 10^7$ and $H = 20$. Two iso-surfaces (A: $T = 0.55$ in blue and $T = 0.8$ in yellow) and interpretation by the plume detection routine (B). Note the cold plume on the right hand side displaying two branches.

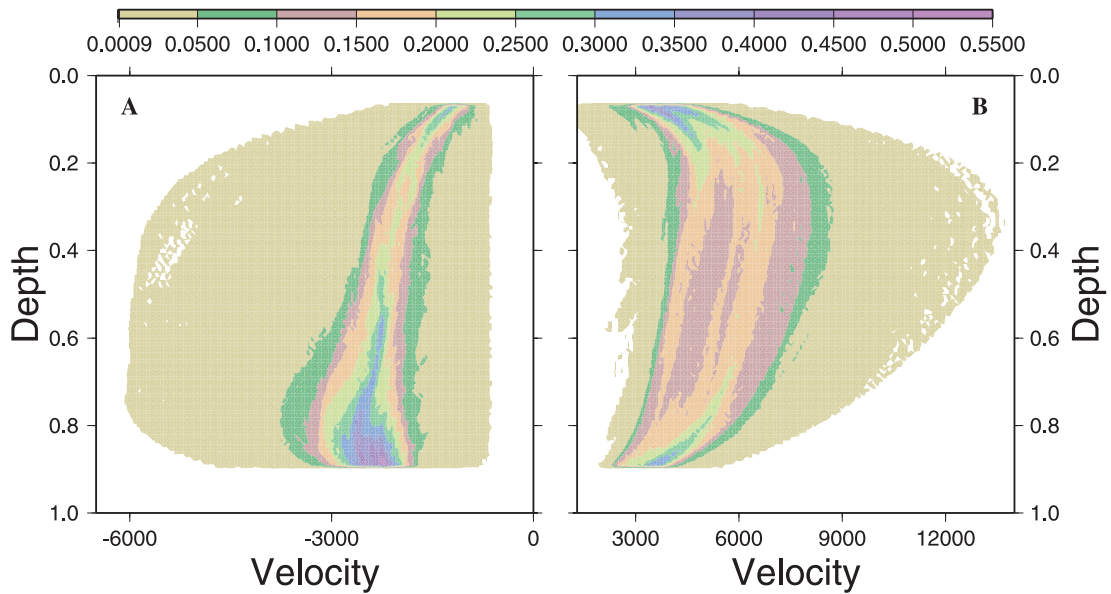


Fig. 2. Distribution (time-averaged over the same period as Fig. 4) of the fluid velocity in hot (A) and cold (B) branches as a function of depth for $Ra = 10^7$, $H = 20$. Positive velocity is downward and the units for the color scale are the number of occurrences at each time step. The largest population of hot plumes starts with a very low velocity and stops halfway to the top of the system whereas the distribution of cold plumes is more regular around its mean value and displays no significant change in the population as a function of depth outside boundary layers.

ter or colder than the average temperature at the same depth. Given a threshold value, all the points that are part of a plume are easily identified at each depth and finding the connected components, a classical image analysis procedure (e.g. [18]), allows the identification of all the plume cross-sections at each depth. The three-dimensional structure of the plumes is then reconstructed by comparing the successive cross-sections. A plume has to be modeled as a tree which may contain several branches, resulting from the interactions between plumes (Fig. 1).

The choice of the threshold value is a matter of concern: a too high value results in missing or breaking in part plumes whereas a too conservative value results in counting artifacts as plumes. A conservative choice is made and artifacts are disqualified using coherence arguments: a plume has to have a radius of the same order as the thickness of the boundary layer from which it originated. After reconstruction, the plumes that are either too small or too large (a situation encountered for hot plumes in high heating rate

cases, when the mean temperature is close to the maximum one) are suppressed.

The threshold values are set for each depth as a fixed proportion between the time-averaged minimum, mean and maximum temperatures at the same depth (Fig. 3). More precisely, given the temperature $T(x, y, z)$, the considered point is part of a hot plume if:

$$T(x, y, z) > thr_h(z) = T_{\text{mean}}(z) + p_h [T_{\text{max}}(z) - T_{\text{mean}}(z)] \quad (1)$$

or part of a cold plume if:

$$T(x, y, z) < thr_c(z) = T_{\text{mean}}(z) - p_c [T_{\text{min}}(z) - T_{\text{mean}}(z)] \quad (2)$$

The proportions p_h and p_c for the hot and cold plumes can be different but are chosen independent of depth. To allow error estimates, several different proportions are used at the same time

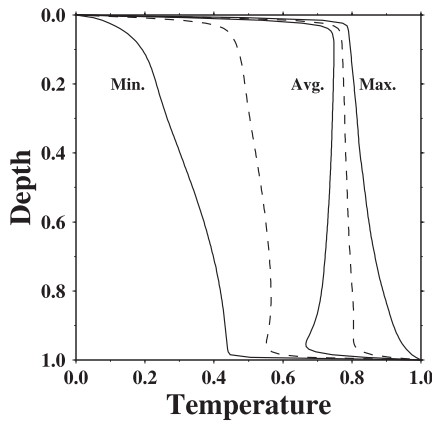


Fig. 3. Minimum, averaged and maximum temperature profiles (solid lines) in the convective system for $Ra=10^7$ and $H=20$. Temperature and depth are given in non-dimensional units. The profiles are averaged for a sufficient time before their use in the plume detection routine. 50% thresholds for cold and hot plume detection are also plotted with dashed lines. Note that the buoyancy available for cold plumes is much larger than that available for hot plumes. Note also that a local minimum outside the bottom boundary layer due to spreading of cold plume heads [7] provides a small additional buoyancy for starting hot plumes but that the overall mean temperature profile in the central part of the system is stabilizing.

and comparison of the results shows that they are similar (within the quantification error) in terms of detection for proportions between 40% and 60%. However, the integrated dynamical characteristic (velocity and advection in the plumes) depends quantitatively on the threshold value, as discussed below.

In Fig. 1 the interpretation of the temperature field by the plume detection routine with a threshold value of 50% is represented in the right panel. It clearly shows that the plume detection routine recovers correctly the plumes in the system.

Once the plumes have been detected, one can compute many of their geometrical (position, average radius, horizontal elongation and vertical extents) and dynamical (average velocity and advection) features. This has been done in real time during the model evolution for $Ra=10^7$ and $H=20$. Fig. 4 displays the number of hot and cold plumes and branches and their maximum and average vertical extent as a function of time. Also represented is the number of plumes at each time that reach the boundary opposite to where they started. One can see that hot and cold plumes behave differently: cold plumes always reach the bottom boundary whereas hot

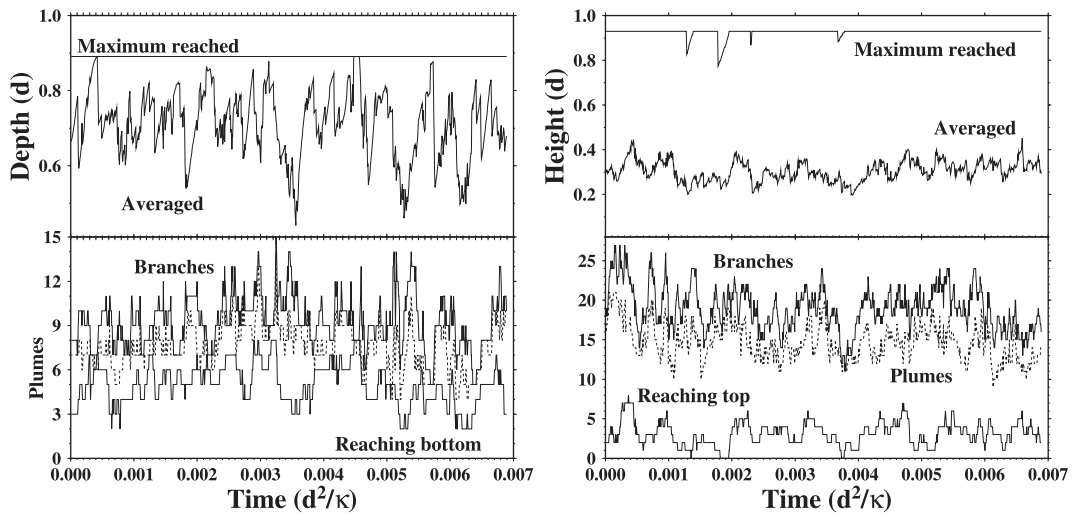


Fig. 4. Number of cold (left bottom) and hot (right bottom) plumes and average and maximum depth (left top) and height (right top) they reach, as a function of time for $Ra=10^7$ and $H=20$. The bottom plots represent the number of branches (top line), plumes (dashed line), and the total number of branches that, at each time step, reach the boundary opposite to where they originated (lowest curve).

plumes, by far the more numerous, seldom make their way to the top boundary. The fact that the average depth cold plume reach is not exactly the maximum depth comes from the fact that there is always one on its way to the bottom boundary.

Many hot plumes start because there is a local minimum in the average temperature profile just outside the bottom boundary layer due to the spreading of cold plume heads [7] (Fig. 3). This provides a buoyancy source leading to small instabilities but is not enough to overcome the stable temperature gradient in the core of the system which is observed in internally heated Rayleigh–Bénard convection [6,7,19]. Cold plume heads also help to start small hot plumes by mechanically pushing and concentrating hot matter. It is particularly evident, in Fig. 1 and the different animations that have been made, that the position of the thermal instabilities in the bottom boundary layer, hence of hot plumes, is controlled by cold plumes. Thermal instabilities in the boundary layer are linear and mostly shaped by the spreading of cold plume heads, and from these linear instabilities plumes are formed. This process, termed the instability from tabular up-welling to plume by Sleep et al. [15], leads to weak hot plumes that do not reach the top surface. The plumes that do reach the top surface originate from the intersection of two or three linear (tabular) instabilities where there is constructive interaction between different buoyancy sources.

On the other hand, there is no marked local maximum below the top boundary layer showing that it is not significantly affected by hot plumes so that all the cold plumes starting are buoyant enough to reach the bottom plate.

Histograms of the number of plumes at each time step as a function of depth and fluid velocity in the plume (Fig. 2) show that the largest population of hot plumes starts with a very low velocity and is restricted to the lower half of the system.

3. Heat transfer by plumes

The advection by each plume is computed by integrating $w(T - T_{\text{mean}}(z))$ over each cross-section,

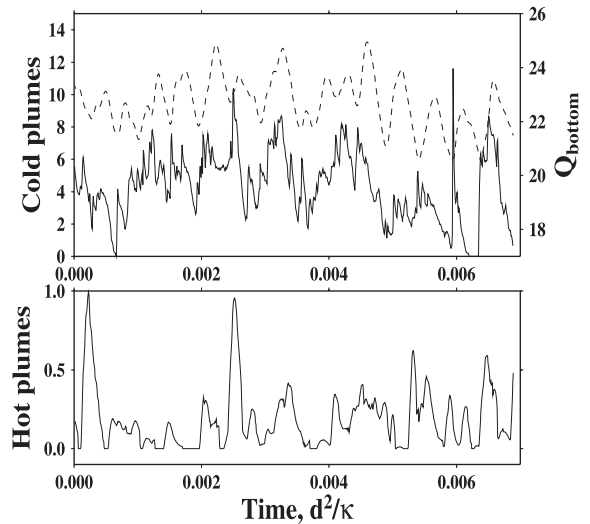


Fig. 5. Advection by plumes and bottom heat flux as a function of time: total advection by hot plumes arriving at the top surface (bottom plot), total advection by cold plumes arriving at the bottom surface (top plot, left scale) and heat flux at the bottom boundary (top plot, dashed line, right scale). Quantitative comparison of advection by plumes and bottom heat flux is not possible since it depends on the choice of threshold for plume detection (here 50%, see text and Fig. 6) but the time evolutions show clearly that the bottom heat flux is controlled by cold plumes arriving rather than hot plumes departing.

w being the vertical velocity. Comparison of the total advection by cold plumes arriving at the bottom plate and the heat flux at the bottom surface (Fig. 5) shows that these two time series are strongly correlated (correlation coefficient of 0.7) whereas the advection by hot plumes arriving at the top surface is totally uncorrelated to the heat flux at the bottom surface (correlation coefficient less than 0.3). This means that the heat flux at the bottom of an internally heated convective system is strongly controlled by down-welling currents rather than by departing hot instabilities. Profiles of advection by cold and hot plumes (Fig. 6) also prove that down-welling currents are the major means of transporting heat in such a system, not only in the central part but also close to the bottom boundary layer.

In Fig. 6 the profiles of total advection as a function of depth and the part of it that can be attributed to up- and down-welling currents, without the use of any threshold, are also represented.

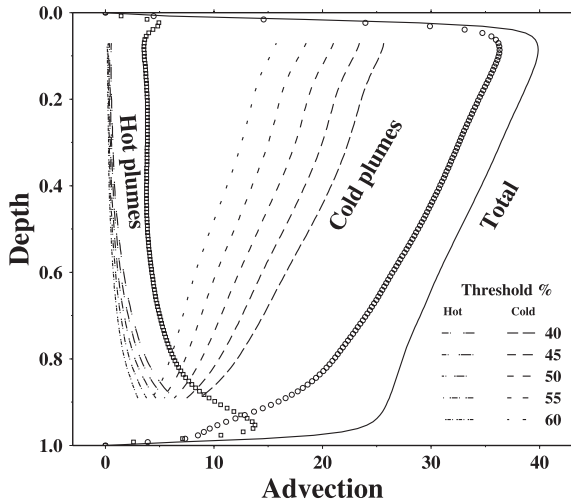


Fig. 6. Heat advection averaged in time and as a function of depth. Total advection is the solid line and the parts due to cold and hot plumes are the dashed and dash-dotted lines, respectively. The circles (squares) represent the part of the advection that is due to a downward (upward) current, without use of any threshold. This allows the computation of the maximum values of advection that could be obtained in the case of an optimum threshold. Different threshold values between 40% and 60% are used, showing that most of the advection is due to cold plumes, even close to the bottom boundary. This statement depends quantitatively on the threshold value but not qualitatively. In the bottom boundary layer, up-welling currents slightly overcome down-welling currents but they are mostly due to the spreading of cold plume heads.

This procedure obviously gives much less information than the plume detection but provides an estimate of the maximum advection by plumes that could be obtained in the case of an optimum threshold. In the case of cold plumes, the fraction f of this maximum that is recovered by the plume detection routine is found to be almost constant with depth and depends on the proportion p_c as $f = 1.25 - 1.5 \times 10^{-2} p_c$. This relation is certainly not valid when p_c tends to zero but it means that all the down-welling advection can be entirely attributed to cold plumes and that the quantitative difference observed in Fig. 5 between the advection by cold plumes and the bottom heat flow can be attributed to the truncation by the plume detection routine.

On the other hand, the advection by hot plumes in the upper half of the system does not converge

to the total up-welling advection when the threshold is decreased and the largest part of this advection does not depend on depth and can be attributed to the diffuse return flow that is observed in internally heated convection [6]. The advection by plumes is only significant in the lower half of the system where it is helped by the arrival of cold plume heads.

The heat flux at the top boundary of the system has been found to scale as $q_{\text{top}} \propto \text{Ra}^\beta \Delta T_{\text{top}}^{\beta+1}$, ΔT_{top} being the temperature jump across the top boundary layer and the exponent β being close to 1/3 [7,20]. This result, classical in Rayleigh–Bénard convection, can be explained by the conductive growth of the boundary layer followed by the release of a thermal plume when the boundary layer is too thick to stay stable and a new start of the same cycle [21]. On the other hand, the bottom heat flow has been found to scale as $q_{\text{bot}} \propto \text{Ra}^{1/4} \Delta T_{\text{bot}}$, ΔT_{bot} being the temperature jump across the bottom boundary layer [7,20], a very different result that can be attributed to the effect of cold plumes on the bottom boundary layer.

4. Discussion

The main effect of volumetric heating on Rayleigh–Bénard convection is to break the symmetry between hot and cold structures (e.g. [22]) and to favor down-welling structures over up-welling ones [7,19,23,24] with two major consequences: hot plumes that start from the bottom boundary do not always cross the whole system and heat flux at the lower surface is primarily controlled by the arrival of down-going currents. In the classical view of plumes, the parameter controlling the boundary layer instabilities is the local Rayleigh number, computed using the characteristics of the boundary layer [21]. This local Rayleigh number is related to the heat flow by unit surface. If the heat flux at the top boundary in the present simulation ($Q_{\text{top}} = 43$) is scaled to the heat flux at the surface of the Earth ($q_{\text{Earth}} \approx 40$ TW) [25], the present bottom heat flux ($Q_{\text{bot}} = 23$) would give for the total heat flux at the core–mantle boundary $Q_{\text{CMB}} = R_{\text{CMB}}^2 / R_{\text{Earth}}^2 \times Q_{\text{bot}} / Q_{\text{top}} \times Q_{\text{Earth}} \approx 6.47$

TW. Although the Cartesian system used in the present simulation is heated half from below and half from within, its scaling to spherical geometry gives a value for the CMB heat flow in the middle of the proposed range (e.g. [26,27]). However, several other simulations were run and showed that the present findings do not depend on the exact values of Ra and H , as long as this last parameter is not vanishingly small. A more systematic study is presently conducted to find scaling laws for the different quantities presented here, like the average height reached by hot plumes.

Obviously, the convection model used here is much simpler than the Earth's mantle and a strict application of its finding to the actual mantle remains somewhat speculative. It is thus worth discussing the additional complexities of the mantle that may change the present figure.

The viscosity of the mantle is thought to be highly temperature-dependent and lateral variations of viscosity are indeed necessary to build the toroidal velocity field at the surface of the Earth [28]. Sleep et al. [15] showed that a two orders of magnitude decrease of viscosity across the lower boundary layer of the convecting system was necessary for the formation of plumes at the expense of tabular up-welling. It was shown above that plumes can be formed even in a constant viscosity fluid but that these plumes are weak. In the large viscosity variation scenario, the time needed for a new plume to rise through the high viscosity mantle is large (100 Ma, according to [15]) and the low viscosity plume head is likely to be deformed by the large-scale plate flow during its ascent. In the same line of reasoning, it has been well demonstrated [29] that the hot boundary layer is largely influenced by the arrival of cold down-welling currents in an experiment of convection in a temperature dependent viscosity fluid.

Convection experiments in fluids with highly temperature-dependent viscosity show that the average temperature is higher than in the constant viscosity case and that a stagnant rigid lid then develops at the top boundary where most of the viscosity contrast happens (e.g. [30,31]) so that a contrast of less than about 20 could be expected across the bottom boundary layer [32]. A way out

of this is to have the lid move and subduct so that its arrival and spreading at the bottom boundary provide a temperature and viscosity contrast helping the formation of hot plumes. This process was proposed by Nataf [32] and his fig. 5 displays a local temperature drop above the bottom boundary layer that is similar to the one of Fig. 3 (see also [33]). From this model, it can also be expected that the bottom heat flux will be dominated by the arrival of cold and stiff plates. In the three-dimensional mantle, plates are two-dimensional objects so that their volume is considerably more important than plumes. It has to be expected that plates will dominate heat transfer even more than cold plumes do in the present model. In other words, the temperature dependence of viscosity and the existence of large-scale plate flow [34] should enhance the conclusion of the present paper that the heat flux at the CMB is controlled by down-welling currents rather than departing hot plumes. Moreover, a causal link between the arrival of cold down-welling currents at the bottom boundary and the formation of hot plumes, which is observed in the present constant viscosity model, should also be enhanced in the presence of high viscosity plates [32]. The extension of the present results to a model of convection with self-consistent formation of plates [35] is currently being performed (Labrosse and Tackley, in preparation).

Obviously, cavity plumes with a large head and a thin tail [36] that have been proposed as an origin for the largest hotspot chains [37] cannot be obtained in a constant viscosity simulation. However, this model seems to explain only four of the many hotspot tracks that are evidenced on the Pacific Plate [38]. The remaining seamounts could be either of shallow origin [39] or the surface expression of short-lived and weak plumes that are easily obtained in high Rayleigh number internally heated convection.

The question of the apparent plume stability in mantle convection also deserves some discussion. The plumes that are obtained in the present iso-viscous model are highly time-dependent. It has been argued that an increase of viscosity with depth in the mantle was one way to stabilize mantle plumes. Steinberger and O'Connell [40]

showed that the advection of plume conduit by large-scale flow leads to the observed small hot-spot motion if the viscosity increases strongly with depth in the lower mantle. This question may be of importance since the effect of down-welling currents will decrease with depth like the inverse square root of viscosity. However, inferring large radial variations of the viscosity from models that do not allow lateral variations [40] is highly questionable [41] since viscosity is thought to vary by several orders of magnitude with temperature but only mildly with pressure [42] in the absence of chemical stratification. The variation of viscosity with pressure is then likely to modify the proportions of the heat flux at the CMB that are due to plates and hot plumes but not to the point of reversing it.

Another option to explain the apparent fixity of mantle plumes is by tying their sources to a chemical heterogeneity at the base of the mantle, which may provide the increase of viscosity needed for plume stability. This heterogeneity could take the form of a continuous layer [43] or discontinuous piles [44] or even crypto-continentals [45,46], and in any case would have an important topography that could be at the origin of the two superswells [43]. In this model, the mantle plumes at the origin of the large stable hotspots come from the summits of the domes and not from the CMB. Therefore, their buoyancy flux cannot give us information on the heat flux out of the core. On the other hand, the strong subducting plates could well be able to deform the chemical interface and shape the domes, as can be assumed from the relative position of the two superswells and the major circum-Pacific subduction.

Overall, the fact that internal heat generation favors down-welling currents over up-welling ones agrees well with the fact that, despite recent progress (see [47] for a review), hot plumes have not been imaged by tomography down to the CMB as convincingly as down-going slabs (e.g. [48]). This means that heat flux out of the hotspots can only be taken as a lower bound for the heat flux at the CMB and to obtain a better estimate of this latter quantity, advection by plates arriving at the CMB must be computed. It also means that a change in the plate flow is more

likely to affect the dynamics of the core, as proposed by [49], than the departure of a hot plume [50,52].

Acknowledgements

I am pleased to thank Ed Kaminski, A. Davaille and C. Jaupart for fruitful discussion about plumes and convection and P. Tackley for his comments on the first draft of this paper. The review by Norm Sleep helped to considerably sharpen the paper. Suggestions about image analysis tools by S. Andréfouët and discussions with M. Holschneider were much appreciated. P. Stoclet provided a parallel routine for real-time iso-surface computation (Fig. 1) and the rest of the figures were done using the Generic Mapping Tools, developed by Wessel and Smith [51]. The CPU time for this study was provided by the Département de Modélisation Physique et Numérique of IPGP and by the Centre Informatique National de l'Enseignement Supérieur (CINES). This is IPGP contribution No. 1803. *[AC]*

References

- [1] W. Morgan, Convection plumes in the lower mantle, *Nature* 230 (1971) 42–42.
- [2] D.E. Loper, F.D. Stacey, The dynamical and thermal structure of deep mantle plumes, *Phys. Earth Planet. Inter.* 33 (1983) 304–317.
- [3] F.D. Stacey, D.E. Loper, The thermal boundary-layer interpretation of D'' and its role as a plume source, *Phys. Earth Planet. Inter.* 33 (1983) 45–55.
- [4] G.F. Davies, Ocean bathymetry and mantle convection, 1. large-scale flow and hotspots, *J. Geophys. Res.* 93 (1988) 10467–10480.
- [5] N.H. Sleep, Hotspots and mantle plumes: some phenomenology, *J. Geophys. Res.* 95 (1990) 6715–6736.
- [6] E.M. Parmentier, C. Sotin, B.J. Travis, Turbulent 3-D thermal convection in an infinite-Prandtl-number, volumetrically heated fluid: implications for mantle dynamics, *Geophys. J. Int.* 116 (1994) 241–251.
- [7] C. Sotin, S. Labrosse, Three-dimensional thermal convection of an isoviscous, infinite-Prandtl-number fluid heated from within and from below: applications to heat transfer in planetary mantles, *Phys. Earth Planet. Inter.* 112 (1999) 171–190.
- [8] E.M. Parmentier, C. Sotin, Three-dimensional numerical experiments on thermal convection in a very viscous fluid:

- Implications for the dynamics of a thermal boundary layer at high Rayleigh number, *Phys. Fluids* 12 (2000) 609–617.
- [9] R.W. Griffiths, I.H. Campbell, Stirring and structure in mantle starting plumes, *Earth Planet. Sci. Lett.* 99 (1990) 66–78.
- [10] E. Moses, G. Zocchi, A. Libchaber, An experimental study of laminar plumes, *J. Fluid Mech.* 251 (1993) 581–601.
- [11] P. Olson, G. Schubert, C. Anderson, Structure of axisymmetric mantle plumes, *J. Geophys. Res.* 98 (1993) 6829–6844.
- [12] D.L. Coulliette, D.E. Loper, Experimental, numerical and analytical models of mantle starting plumes, *Phys. Earth Planet. Inter.* 92 (1995) 143–167.
- [13] B.D. Malamud, D.L. Turcotte, How many plumes are there?, *Earth Planet. Sci. Lett.* 174 (1999) 113–124.
- [14] G.F. Davies, Cooling the core and mantle by plume and plate flows, *Geophys. J. Int.* 115 (1993) 132–146.
- [15] N.H. Sleep, M.A. Richards, B.H. Hager, Onset of mantle plumes in the presence of preexisting convection, *J. Geophys. Res.* 93 (1988) 7672–7689.
- [16] S. Chandrasekhar, *Hydrodynamic and Hydromagnetic Stability*, Oxford University Press, Oxford, 1961.
- [17] C. Lemery, Y. Ricard, J. Sommeria, A model for the emergence of thermal plumes in Rayleigh-Bénard convection at infinite Prandtl number, *J. Fluid Mech.* 414 (2000) 225–250.
- [18] J.-M. Chassery, A. Montanvert, *Géométrie Discrète en analyse d'images. Traité des Nouvelles Technologies, Série Images*, Hermes, Paris, 1991.
- [19] D.P. McKenzie, J.M. Roberts, N.O. Weiss, Convection in the earth's mantle: towards a numerical simulation, *J. Fluid Mech.* 62 (1974) 465–538.
- [20] S. Labrosse, Contribution à l'étude du refroidissement de la Terre, Ph.D. Thesis, Université Paris-7, Denis Diderot, Paris, 1997.
- [21] L.N. Howard, Convection at high Rayleigh number, in: H. Gortler (Ed.), *Proceedings of the Eleventh International Congress of Applied Mechanics*, Springer-Verlag, New York, 1964, pp. 1109–1115.
- [22] T. Yanagisawa, Y. Hamano, 'Skewness' of S-wave velocity in the mantle, *Geophys. Res. Lett.* 26 (1999) 791–794.
- [23] D. Bercovici, G. Schubert, G.A. Glatzmaier, Influence of heating mode on three-dimensional mantle convection, *Geophys. Res. Lett.* 16 (1989) 617–620.
- [24] G. Houseman, The dependence of convection plattform on mode of heating, *Nature* 172 (1988) 297–298.
- [25] J.G. Sclater, C. Jaupart, D. Galson, The heat flow through oceanic and continental crust and the heat loss of the Earth, *Rev. Geophys. Space Phys.* 18 (1980) 269–312.
- [26] S. Labrosse, J.-P. Poirier, J.-L. Le Mouél, On cooling of the Earth's core, *Phys. Earth Planet. Inter.* 99 (1997) 1–17.
- [27] S. Labrosse, J.-P. Poirier, J.-L. Le Mouél, The age of the inner core, *Earth Planet. Sci. Lett.* 190 (2001) 111–123.
- [28] Y. Ricard, C. Vigny, Mantle dynamics with induced plate-tectonics, *J. Geophys. Res.* 94 (1989) 17543–17559.
- [29] N. Schaffer, M. Manga, Interaction of rising and sinking mantle plumes, *Geophys. Res. Lett.* 28 (2001) 455–458.
- [30] H.-C. Nataf, F.M. Richter, Convection experiments in fluids with highly temperature-dependent viscosity and the thermal evolution of the planets, *Phys. Earth Planet. Inter.* 29 (1982) 320–329.
- [31] A. Davaille, C. Jaupart, Transient high-Rayleigh-number thermal convection with large viscosity variations, *J. Fluid Mech.* 253 (1993) 141–166.
- [32] H.-C. Nataf, Mantle convection, plates and hotspots, *Tectonophysics* 187 (1991) 361–371.
- [33] A. Lenardic, W.M. Kaula, Tectonic plates, D'' thermal structure, and the nature of mantle plumes, *J. Geophys. Res.* 99 (1994) 15697–15708.
- [34] A.M. Jellinek, H.M. Gonnermann, M.A. Richards, Plume capture by divergent plate motions: Implications for the distribution of hotspots, geochemistry of mid-ocean ridge basalts and heat flux at the core-mantle boundary, *Earth Planet. Sci. Lett.* (2002) submitted.
- [35] P.J. Tackley, Self-consistent generation of tectonic plates in time-dependent, three-dimensional mantle convection simulations 1. pseudoplastic yielding, *Geochem. Geophys. Geosyst.* 1 (2000) 2000GC000036.
- [36] P. Olson, H. Singer, Creeping plumes, *J. Fluid Mech.* 158 (1985) 511–531.
- [37] M.A. Richards, R.A. Duncan, V.E. Courtillot, Flood basalts and hot-spot tracks: Plume heads and tails, *Science* 246 (1989) 103–107.
- [38] V. Clouard, A. Bonneville, How many Pacific hotspots are fed by deep mantle plumes?, *Geology* 29 (2001) 695–698.
- [39] D.L. Anderson, The thermal state of the upper mantle; no role for mantle plumes, *Geophys. Res. Lett.* 27 (2000) 3623–3626.
- [40] B. Steinberger, R.J. O'Connell, Advection of plumes in mantle flow: Implications for hotspot motion, mantle viscosity and plume distribution, *Geophys. J. Int.* 132 (1998) 412–434.
- [41] Z. Martinec, O. Čadež, L. Fleitout, Can the 1D viscosity profiles inferred from postglacial rebound data be affected by lateral viscosity variations in the tectosphere?, *Geophys. Res. Lett.* 28 (2001) 4403–4406.
- [42] D. Yamazaki, S.-I. Karato, Some mineral physics constraints on the rheology and geothermal structure of Earth's lower mantle, *Am. Mineralog.* 86 (2001) 385–391.
- [43] A. Davaille, Hotspots, superswells and mixing in a heterogeneous mantle, *Nature* 402 (1999) 756–760.
- [44] P.J. Tackley, Three-dimensional simulations of mantle convection with a thermochemical CMB boundary layer: D''?, in: M. Gurnis, M.E. Wyession, E. Knittle, B.A. Buffett (Eds.), *The Core-Mantle Boundary Region*, American Geophysical Union, Washington, DC, 1998, pp. 231–253.
- [45] F.D. Stacey, Effects on the core of structure within D'', *Geophys. Astrophys. Fluid Dyn.* 60 (1991) 157–163.
- [46] A. Namiki, K. Kurita, The influence of boundary heterogeneity in experimental models of mantle convection with

- internal heat sources, *Phys. Earth Planet. Inter.* 128 (2001) 195–205.
- [47] H.-C. Nataf, Seismic imaging of mantle plumes, *Annu. Rev. Earth Planet. Sci.* 28 (2000) 391–417.
- [48] R.D. van der Hilst, S. Widiyantoro, E.R. Engdahl, Evidence for deep mantle circulation from global tomography, *Nature* 386 (1997) 578–584.
- [49] Y. Gallet, G. Hulot, Stationary and nonstationary behaviour within the geomagnetic polarity time scale, *Geophys. Res. Lett.* 24 (1997) 1875–1878.
- [50] R.L. Larson, P. Olson, Mantle plumes control magnetic reversal frequency, *Earth Planet. Sci. Lett.* 107 (1991) 437–447.
- [51] P. Wessel, W.H.F. Smith, New, improved version of generic mapping tools released, *EOS Trans. Am. Geophys. Union* 79 (1998) 579.
- [52] V. Courtillot, J. Besse, Magnetic-field reversals, polar wander and core-mantle coupling, *Science* 237 (1987) 1140–1147.